Nuclear F-actin Cytology in Oral Epithelial Dysplasia and Oral Squamous Cell Carcinoma

M.P. McRae[1] iD**, A.R. Kerr[2], M.N. Janal[3], M.H. Thornhill[4]** iD**, S.W. Redding[5], N. Vigneswaran[6], S.K. Kang[7], R. Niederman[8], N.J. Christodoulides[1], D.A. Trochesset[2], C. Murdoch[4]** iD**, I. Dapkins[9], J. Bouquot[10], S.S. Modak[1], G.W. Simmons[1], and J.T. McDevitt[1]**

Abstract

Oral cavity cancer has a low 5-y survival rate, but outcomes improve when the disease is detected early. Cytology is a less invasive method to assess oral potentially malignant disorders relative to the gold-standard scalpel biopsy and histopathology. In this report, we aimed to determine the utility of cytological signatures, including nuclear F-actin cell phenotypes, for classifying the entire spectrum of oral epithelial dysplasia and oral squamous cell carcinoma. We enrolled subjects with oral potentially malignant disorders, subjects with previously diagnosed malignant lesions, and healthy volunteers without lesions and obtained brush cytology specimens and matched scalpel biopsies from 486 subjects. Histopathological assessment of the scalpel biopsy specimens classified lesions into 6 categories. Brush cytology specimens were analyzed by machine learning classifiers trained to identify relevant cytological features. Multimodal diagnostic models were developed using cytology results, lesion characteristics, and risk factors. Squamous cells with nuclear F-actin staining were associated with early disease (i.e., lower proportions in benign lesions than in more severe lesions), whereas small round parabasal-like cells and leukocytes were associated with late disease (i.e., higher proportions in severe dysplasia and carcinoma than in less severe lesions). Lesions with the impression of oral lichen planus were unlikely to be either dysplastic or malignant. Cytological features substantially improved upon lesion appearance and risk factors in predicting squamous cell carcinoma. Diagnostic models accurately discriminated early and late disease with AUCs (95% CI) of 0.82 (0.77 to 0.87) and 0.93 (0.88 to 0.97), respectively. The cytological features identified here have the potential to improve screening and surveillance of the entire spectrum of oral potentially malignant disorders in multiple care settings.

Keywords: artificial intelligence, biomarkers, point-of-care testing, single-cell analysis, cell biology, actins

[1]Department of Biomaterials, Bioengineering Institute, New York University College of Dentsitry, New York, NY, USA

[2]Department of Oral and Maxillofacial Pathology, Radiology & Medicine, New York University College of Dentistry, New York, NY, USA

[3]Department of Epidemiology and Health Promotion, New York University College of Dentistry, New York, NY, USA

[4]Department of Oral & Maxillofacial Medicine, Surgery and Pathology, School of Clinical Dentistry, University of Sheffield, Sheffield, UK

[5]Department of Comprehensive Dentistry and Mays Cancer Center, The University of Texas Health Science Center at San Antonio, San Antonio, TX, USA

[6]Department of Diagnostic and Biomedical Sciences, The University of Texas Health Science Center at Houston, Houston, TX, USA

[7]Departments of Radiology, Population Health New York University School of Medicine, New York, NY, USA

[8]Department of Epidemiology and Health Promotion, New York University, New York, NY, USA

[9]Departments of Population Health and Medicine, New York University School of Medicine, New York, NY, USA

[10]Department of Diagnostic and Biomedical Sciences, The University of Texas School of Dentistry at Houston, Houston, TX, USA

Corresponding Author:
J.T. McDevitt, Department of Biomaterials, Bioengineering Institute, New York University, 433 First Avenue, New York, NY 10010-4086, USA.
Email: mcdevitt@nyu.edu

Introduction

Oral potentially malignant disorders (OPMDs) are clinical diagnoses rendered when a clinician encounters a lesion that cannot be attributed to a benign origin. These lesions require further diagnostic testing to rule out oral epithelial dysplasia (OED) or oral squamous cell carcinoma (OSCC). The typical pathway to OPMD diagnosis is biopsy and histopathologic evaluation requiring a specialty referral and invasive surgical procedure. Given the overlapping clinical features encountered by dentists, it is challenging to perform a risk assessment based on lesion appearance and risk factors alone and decide whether referral is required (Lingen et al. 2017). Although there are numerous minimally invasive adjuncts to assist in OPMD triage, only cytology has been demonstrated as an accurate surrogate for histopathology (Rashid and Warnakulasuriya 2015; Lingen et al. 2017; Huber 2018). However, delays associated with remote laboratory testing and bias of previous studies (Svirsky et al. 2002; Poate et al. 2004) have hindered the adoption of cytology adjuncts. There is a strong need for adjunctive testing in near real-time at the point of care (POC) with sufficient sensitivity to identify at-risk lesions and sufficient specificity to discriminate benign lesions.

Cytological signatures are morphological, phenotypical, or intensity-based measurements from images of stained cells that may be of clinical and diagnostic utility. Cell phenotypic changes involving cytoskeletal actin have been associated with cancer initiation and progression (Gunning et al. 2008; Stevenson et al. 2012). Cancer cells require a high degree of cellular motility to invade, spread, and grow—processes that are driven by actin polymerization, cell adhesion, and actin-myosin contraction (Olson and Sahai 2009). Actin content has shown strong promise as a biomarker for OSCC (de Jong et al. 2010). Previous studies have implicated nuclear actin in a variety of functions, such as supporting and organizing nuclear content (Belin et al. 2013), mechanosensing (Le et al. 2016), nuclear expansion (Moore and Vartiainen 2017), and increasing nuclear compliance while maintaining mechanical protection for genetic material (Miroshnikova et al. 2017). Early studies of in vitro cellular transformation models showed promise for nuclear actin biomarkers for bladder cancer risk assessment in uroepithelial cell lines (Hemstreet et al. 1996). Although promising basic scientific research has advanced the understanding of such cytological signatures, their translational diagnostic utility has not yet been demonstrated for OED or OSCC. Multimodal models incorporating cytological signatures including actin, features of lesion appearance, and risk factors have strong potential to improve diagnostic performance.

Previously, we reported a cytology-on-a-chip system comprising microfluidics, multispectral fluorescence imaging, and single-cell analytics (Weigum et al. 2010). The approach was validated through a multisite clinical validation effort in which brush cytology measurements were correlated with 6 levels of histopathological diagnosis (Speight et al. 2015; Abram et al. 2016). Recently, we developed a POC oral cytology tool comprising a brush cytology test kit, cartridge, instrument, clinical algorithms, and software that automates analysis of cytological signatures of OED and OSCC in a matter of minutes (McRae et al. 2020). Although diagnostic accuracy for the cytology-on-a-chip rivaled and exceeded commercially available adjuncts (Svirsky et al. 2002; Poate et al. 2004; Pereira et al. 2016), additional studies were needed to investigate the clinical utility of novel cytological signatures of OED and OSCC. The current study aimed to determine whether novel cytological signatures identified by machine learning could provide diagnostic utility for OED and OSCC. Here, we describe a retrospective analysis of cytology data and hypothesize whether diagnostic signatures, including cytological features related to F-actin localization, could predict OED and OSCC in clinical applications such as OPMD triage in primary care and OED/OSCC surveillance in secondary or tertiary care settings.

Materials and Methods

Study Design and Participants

A cytology-on-a-chip system was evaluated for its ability to classify mucosal lesions according to histopathologic diagnosis in a cross-sectional study of prospectively recruited subjects seeking care at oral medicine, oral surgery, or otolaryngology clinics. The study was conducted through consecutive sampling at 4 sites. The study was approved by the institutional review boards of all participating institutions. All participants were 18 y and older and were willing and able to participate and provide informed consent. Histopathological and brush cytological samples were collected from 999 patients and assigned into 3 groups: (1) prospectively recruited patients with OPMD who underwent scalpel biopsy as part of standard of care, (2) patients with recently diagnosed OSCC, and (3) healthy volunteers without lesions. Group 1 subjects were eligible if they were diagnosed with OPMD for which a conventional biopsy was indicated and the lesion was at least 5 mm in diameter. Scalpel biopsies were subsequently performed as part of standard of care. Group 2 subjects were eligible if they were diagnosed with a malignant lesion by incisional biopsy within 45 d of the enrollment visit, the remaining lesion was large enough to allow brushing at least 5 mm away from the incisional biopsy site, and area of the lesion available for brushing was at least 5 mm in diameter (i.e., brush sampling was performed after scalpel biopsy). Group 3 subjects were healthy volunteers recruited with normal-appearing oral mucosa and had brush samplings of the tongue and buccal mucosa.

Histopathological diagnosis categorized scalpel biopsy specimens into 6 categories based on the WHO guidelines (El-Naggar et al. 2017) plus healthy controls without lesions who did not undergo scalpel biopsy (Appendix Table 1). A new adjudication process (Speight et al. 2015) was implemented to overcome limitations of conventional OED grading (Warnakulasuriya et al. 2008). Adjacent serial histologic sections were independently scored by 2 pathologists. Two consecutive serial sections were prepared and scored by 2 pathologists blinded to the clinical and microscopic diagnosis and site of the lesion. The pathologists were senior and experienced oral and maxillofacial pathologists (see Acknowledgments for the list
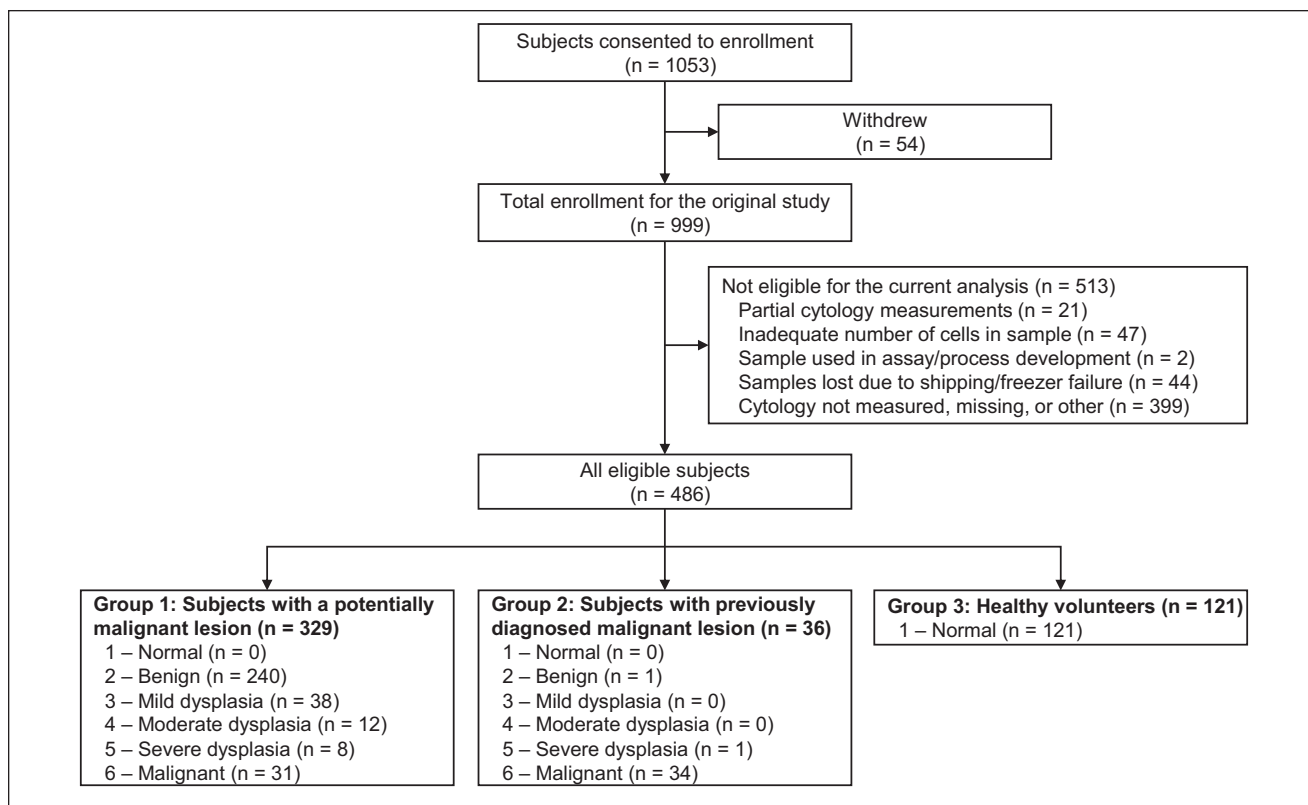
Figure 1. Flow of study participants.

of pathologists). Upon disagreement of scoring, a third independent pathologist reviewed both sections (J.B.). This adjudicator was independent of the previous review stages and blinded to clinical details, original diagnoses, and opinions of Reviewers 1 and 2. If the adjudicator did not agree with either of the initial 2 pathologists, a third-stage consensus review was conducted to attain a final diagnosis. All subjects with sufficient material and complete biomarker results were included in the analysis.

Procedures

Using a procedure standardized across all sites, brush cytology samples were collected with a soft Rovers Orcellex brush according to the manufacturer's instructions (Rovers Medical Devices B.V.) and applied directly to the lesion or control oral mucosa using moderate pressure and rotated 360° approximately 10 to 15 times in the same direction. Immediately after brush cytology samples were collected, cells were harvested by vortexing the brush head in minimum essential medium (MEM) culture media; this was followed by a phosphate-buffered saline (PBS) wash, resuspension in fetal bovine serum (FBS) containing 10% dimethyl-sulfoxide (DMSO), freezing, and storage in a −80°C freezer. Upon processing, samples were thawed rapidly in a 37°C water bath, washed with PBS, and fixed for 1 h in 0.5% formaldehyde. After fixation, cells were washed twice in PBS, resuspended in 150 μL of 0.1% PBS

with 0.1% bovine serum albumin (PBSA), and stored at 4°C until ready to process. Before sample delivery, the cell suspension was diluted in a 20% glycerol/0.1% PBSA solution. A working concentration of 0.33 μM was used for Phalloidin-AlexaFluor-647 (Life Technologies #A22287) and 5 μM for DAPI (Life Technologies #D3571). The cytology-on-a-chip device was primed with PBS at 735 μL/min for 2 min. A cell suspension (20% glycerol, 0.1% PBSA) was flowed at 1.5 mL/min for 2 min such that cells were captured on a nanoporous membrane. The cells were washed with PBS (1 mL/min for 2.5 min). Primary antibody was delivered at 250 μL/min for 2.5 min. The cells were washed again with PBS. Secondary antibody was delivered at 250 μL/min for 2.5 min. A final wash was performed with PBS. Cytology assays had on average 2,000 cells per measurement. Assays that resulted in no cells or very few cells on the membrane were repeated until the cytology sample was depleted.

Cell Phenotype Classifier

Classifiers were trained to identify and quantify cellular and nuclear phenotypes: differentiated squamous epithelial (DSE) cells, small round (SR) cells, mononuclear leukocytes (ML), lone nuclei (LN), and DSE cells with (NA+) and without (NA−) nuclear F-actin. *k*-Nearest Neighbor algorithms were trained on a subset of 144 features from cytology, including morphological and intensity-based measurements. Principal

Table 1. Subject Characteristics.

Characteristic	*N* (%)
Total	486
Sex	
Male	211 (43.4)
Female	275 (56.6)
Age	
≤60 y	321 (66.0)
>60 y	165 (34.0)
Tobacco	
Never	213 (43.8)
Any tobacco use	273 (56.2)
Previous smokers	140 (28.8)
Current smokers	113 (23.3)
Average pack years in tobacco users	13 (1.8 to 30.0)
Subject group	
Healthy volunteer	121 (24.9)
Patients with previously diagnosed malignant lesion	36 (7.4)
Patients with a potentially malignant lesion	329 (67.7)
Lesion characteristics	
No lesion	121 (24.9)
Lesion	365 (75.1)
Diameter	
5 to 10 mm	97 (20.0)
10 to 20 mm	103 (21.2)
≥20 mm	124 (25.5)
Diffuse lesion	41 (8.4)
Color	
Red	56 (11.5)
White	135 (27.8)
Red and white	170 (35.0)
Clinical impression of lichen planus	101 (20.8)
Location	
Floor of mouth	24 (4.9)
Gingiva	63 (13.0)
Hard palate	10 (2.1)
Buccal mucosa	122 (25.1)
Upper or lower lip	16 (3.3)
Soft palate	24 (4.9)
Tongue	106 (21.8)
Histopathological diagnosis	
1—Normal	121 (24.9)
2—Benign	241 (49.6)
3—Mild dysplasia	38 (7.8)
4—Moderate dysplasia	12 (2.5)
5—Severe dysplasia	9 (1.9)
6—Malignant	65 (13.4)

Histopathological diagnoses were based on the WHO classification (El-Naggar et al. 2017). Average pack-years is the average number of cigarettes smoked per day times years smoked divided by 20 (interquartile range).

component analysis was performed on the training set to improve data visualization. The cell phenotyping algorithms were applied across all cytological measurements, and the proportions of each phenotype were compared for each lesion class.

Model Development and Statistical Analysis

The intended sample size for enrollment was 850 subjects, with the first two-thirds (*n* = 567) for development and the final third (*n* = 283) for validation in order to detect a lower 2-sided 95% confidence limit of area under the curve (AUC) of 0.745 or greater for premalignant versus malignant (true underlying AUC of 0.85) and 0.824 for nonneoplastic versus dysplasia and malignant (true underlying AUC of 0.90) with 90% power. Diagnostic accuracy (AUC, sensitivity, and specificity) was determined between histopathology gradings with case versus noncase (indicated by "|") including models for *early disease*, defined as the distinction of cases with benign lesions from all other more severe lesions (i.e., 2 | 3,4,5,6), and *late disease*, defined as the distinction of cases with lesions of lesser severity from all more severe lesions (i.e., 2,3,4 | 5,6). Univariate and multivariate adjusted odds ratios (OR), 95% confidence intervals, and *P* values (2-tailed) were calculated from logistic regression analyses. Pre- and posttest probabilities were estimated by likelihood ratios for late disease. The predictors included cell phenotype percentages for types NA−, NA+, SR, and ML (log_{10} transformed); sex; age (10-y increments); lesion area (log_{10} transformed); lesion color (red, white, or red and white); clinical impression of oral lichen planus; and smoking pack-years (log_{10} transformed). Lasso logistic regression models were developed, and model responses were evaluated for diagnostic performance.

Results

A total of 1,053 subjects were enrolled in the study (Fig. 1). A total of 54 subjects withdrew from the study. Of the 999 remaining enrolled subjects for the original study, 513 were not eligible for the analysis due to the following reasons: partial cytology measurements were made (*n* = 21); the sample contained an inadequate number of cells (*n* = 47); samples were used for other purposes (*n* = 2); samples were lost due to shipping errors and/or freezer failures (*n* = 44); cytology results were not measured due to funding constraints or samples missing (*n* = 399). The remaining 486 subjects with complete histopathology-matched cytology data were included in the current analysis (Table 1). All measurements were completed with cytology-on-a-chip prototypes that have recently been translated to POC cartridges and instruments (Appendix Fig. 1) (McRae et al. 2020). No adverse events were encountered for either the brush cytology or scalpel biopsy sampling.

Cell phenotype classifiers were trained to identify 5 distinct cellular/nuclear phenotypes (Fig. 2A). DSE cells, or mature keratinocytes, were broad/flat cells 50 to 100 μm in diameter with low nuclear-cytoplasmic (NC) ratio and low cytoplasmic F-actin staining intensity. These cells were further differentiated by the presence (NA+) or absence (NA−) of F-actin localized within or surrounding the nucleus. Immature basaloid keratinocytes (SR) were small circular cells 12 to 30 μm in diameter with high NC ratio and strong cytoplasmic F-actin staining intensity. ML appeared as small, brightly stained pink objects 6 to 23 μm in diameter. LN were objects with DAPI counterstaining, but no cytoplasmic F-actin staining, approximately 5 to 12 μm in diameter.

The latent variable structure of the data was explored with principal components (PC) analysis. Scatter plots show that the data varied along 3 dimensions of cell size (PC1), cytoplasmic

F-actin (PC2), and nuclear F-actin (PC3) (Fig. 2B and C). These PCs account for 33%, 15%, and 14% of variance, respectively, and suggest that cell size and nuclear F-actin content/distribution play an important role in distinguishing cell phenotypes. Cell phenotype distributions varied with lesion severity (Fig. 2D and E). In lesions indicating more advanced disease, NA− cells decreased, and SR and ML cells increased (Wilcoxon rank sum test, $P < 0.05$). Proportion of NA+ cells increased with disease severity ($P < 0.05$) for all diagnostic categories except normal versus benign ($P = 0.53$).

Logistic regression models were developed to discriminate between early and late disease (Appendix Table 2). Early disease refers to the distinction of cases with benign lesions from all other more severe lesions, whereas late disease refers to the distinction of cases with lesions of moderate severity from all more severe lesions. The NA− cells showed a strong protective effect (OR < 1) in both early and late disease univariate models. Similarly, the clinical impression of oral lichen planus was associated with 85% to 90% reduction in the odds of high-grade OED and OSCC. Multivariate models showed some confounding among the predictors. Unique contributors to the early disease model included the presence of NA+ cells, age, and lichen planus. Unique contributors to the late disease model included the presence of SR and ML cells, sex, lesion color, and lesions with the clinical impression of oral lichen planus. These data highlight the unique contribution of cytological analysis to differentiating histopathologically verified diagnoses of OED and OSCC.

Figure 2. Development and application of cellular and nuclear phenotype models. (**A**) Machine learning classifiers were developed to identify 5 phenotypes. Principal components analyses of cellular phenotypes show substantial separation between cellular phenotype labels for (**B**) PC1 versus PC2 and (**C**) PC1 versus PC3, with the majority of the variance explained by cell size (PC1), cytoplasm F-actin (PC2), and nuclear F-actin (PC3). Application of cellular and nuclear phenotype models shows (**D**) distributions of NA−, SR, and ML cells within the study population, representing the predicted mean cell type percentages and 95% CI within each lesion class, and (**E**) distribution of NA+ cells out of all DSE cells. NA− cells are differentiated squamous cells without nuclear F-actin. NA+ cells are differentiated squamous cells with nuclear F-actin. SR cells are small round cells. ML are mononuclear leukocytes. LN are lone nuclei. PC is the principal component. DSE cells are differentiated squamous epithelial cells. *N* is normal lesion (*n* = 121). B is benign lesion (*n* = 241). Mild+Mod is mild and moderate dysplasia (*n* = 50). S+OSCC is severe and oral squamous cell carcinoma (*n* = 74).

Diagnostic performance of a multimodal model was evaluated for various diagnostic cutoffs (Table 2). The predictors included cell phenotype distributions, age, sex, smoking pack-years, lesion area, clinical impression of lesion as oral lichen planus, and lesion color (white, red, or red and white). The lasso logistic regression model responses were numerical values between 0 and 100, and model accuracy was determined at a cutoff value that balanced sensitivity and specificity. All models assigned the correct diagnosis to at least 82% of the sample. Late disease models were more accurate than early disease models. The best models properly assigned 95% of the cases.

The improvement in accuracy attributable to the late disease modeling can be summarized by comparing pre- and posttest likelihood ratios (Akobeng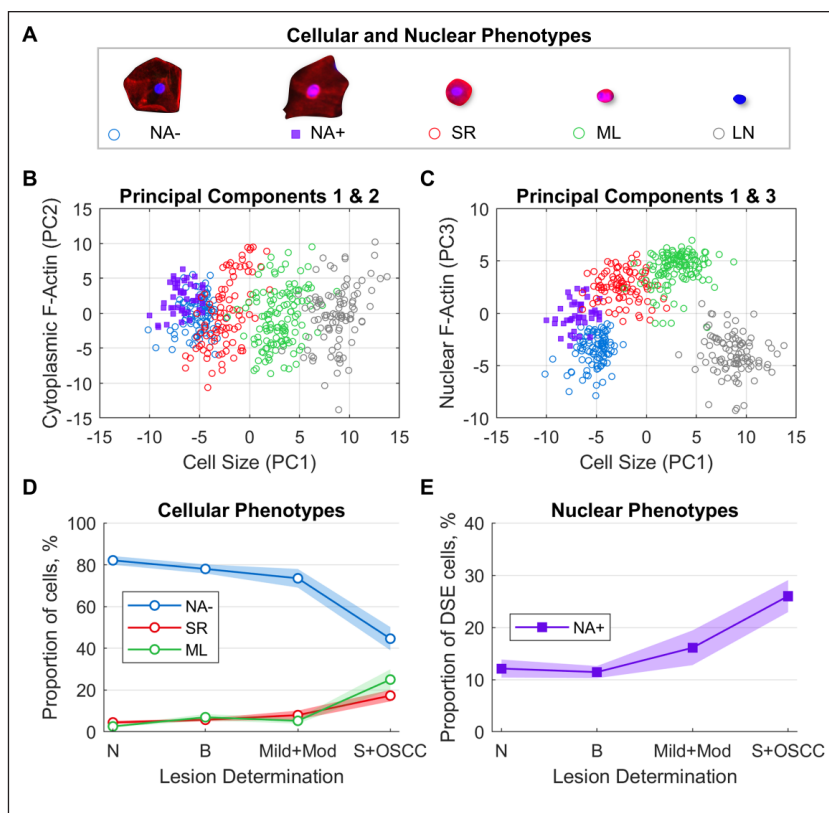 2007). Figure 3 shows the conditional posttest probability for distinguishing patients with late disease as a function of pretest probability for patients with presence or absence of clinical risk factors in the multivariate model. The multivariate model showed the greatest change in posttest probabilities, as indicated by the outermost band of both groups of ellipses. Among the univariate predictors, NA− cells (negative), SR cells (positive), and ML cells (positive) were strongly related to the disease state. Lesions with a white-colored appearance showed a strong protective effect (i.e., the probability of severe dysplasia or OSCC was significantly reduced for those presenting with homogeneous leukoplakia).

Discussion

This study reveals the relative importance of cytological and clinical variables in predicting early and late disease. Significantly, we found that cell phenotype distributions from cytology are

Table 2. OED Spectrum Diagnostic Models.

	Sensitivity	Specificity	AUC
Early disease—2 | 3,4,5,6	0.72 (0.67 to 0.76)	0.73 (0.69 to 0.78)	0.82 (0.77 to 0.87)
2,3 | 4,5,6	0.79 (0.74 to 0.83)	0.85 (0.81 to 0.89)	0.89 (0.84 to 0.93)
WHO binary classification—2,3,4L | 4H,5,6	0.80 (0.75 to 0.84)	0.82 (0.78 to 0.86)	0.89 (0.84 to 0.93)
Late disease—2,3,4 | 5,6	0.86 (0.82 to 0.90)	0.84 (0.80 to 0.88)	0.93 (0.88 to 0.97)
2 versus 6	0.89 (0.85 to 0.92)	0.90 (0.85 to 0.93)	0.95 (0.91 to 0.98)
1 versus 6	0.94 (0.89 to 0.97)	0.92 (0.87 to 0.95)	0.97 (0.94 to 1.00)

Sensitivity, specificity, and area under the curve (AUC) (with 95% confidence interval) are shown for the cross-validated dichotomous algorithms for early disease (2 | 3,4,5,6), mild | moderate dysplasia (2,3 | 4,5,6), WHO binary classification (2,3,4L | 4H,5,6), late disease (2,3,4 | 5,6), benign versus malignant (2 vs. 6), and healthy control versus malignant (1 vs. 6) models.
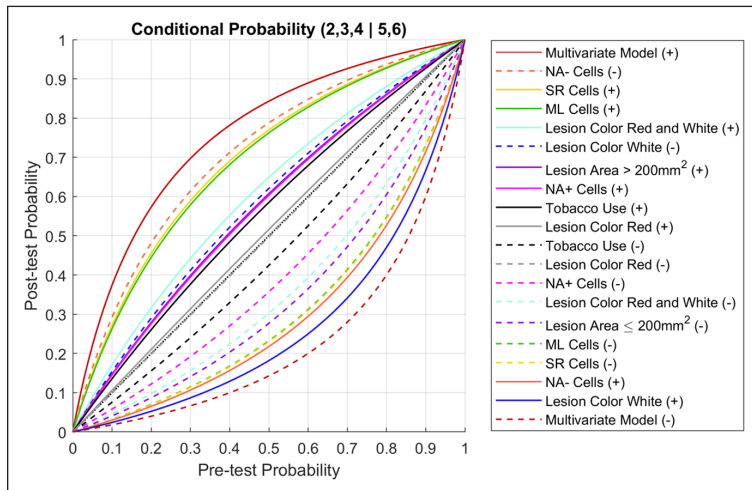
Figure 3. Pre- and posttest probability. Conditional probability plot for late disease (2,3,4 | 5,6). Posttest probabilities are plotted as a function of pretest probability for patients with positive (solid lines) and negative (dashed lines) indications for clinical risk factors (lesion color, lesion area, smoking), cellular phenotypes, and the multivariate model.

strong predictors of disease, and we observed that different cell phenotypes were more important for distinguishing early versus late disease. As expected, SR and ML cells were found to indicate late disease. Small circular cells resembling SR cells were previously found to increase in frequency with OED severity (Babshet et al. 2011). Strong evidence for the association between chronic inflammation and carcinogenesis has been reported previously, which supports the result of elevated numbers of leukocytes in high-grade OED and OSCC (Tampa et al. 2018). Interestingly, the proportion of NA+ cells was a statistically significant factor in predicting early disease. The current study is the first to link increased proportions of nuclear F-actin cells with early OED. It is possible that differentiated squamous cells that develop thick perinuclear/nuclear F-actin formations could represent transitional phenotypes embodying a morphological transformation from NA+ to SR.

Multivariate and multimodal models combining cell phenotypes from cytology, lesion characteristics, and traditional risk factors yielded higher diagnostic utility than any individual predictor. Cytological signatures substantially outperformed clinical features (lesion appearance and risk factors) in predicting OED and OSCC. Although lesion color was a significant

factor in late disease, it was less useful in distinguishing lesions with low malignant potential that are more commonly observed in primary care settings. Although traditional risk factors like tobacco use did not play a dominant role for any OED/OSCC model, the number of smoking pack-years was statistically significant in the benign versus malignant (2 vs. 6) model with OR (95% CI) of 1.97 (1.02 to 3.97). This result further highlights the challenge of lesion diagnosis in a realistic population of patients presenting with intermediate histopathological grading as opposed to extreme comparisons (e.g., healthy control vs. cancer) commonly found in the literature. The clinical impression of oral lichen planus demonstrated a strong protective effect in both early and late disease prediction. Motivated by this result, plans are now in progress to develop a cytological test for lichen planus in primary care settings where the condition may be overlooked or misdiagnosed.

Prior studies of cytology adjuncts had significant methodological gaps that led to overly optimistic results, such as performing matched histopathology on only a subset of lesions with a higher index of suspicion for malignancy (Sciubba 1999; Poate et al. 2004), frequently providing an ambiguous "atypical" result (Svirsky et al. 2002), or comparing only normal or benign versus malignant lesions, excluding a full range of dysplastic lesions (Pereira et al. 2016). In the current study, the cytology-on-a-chip approach was assessed relative to 6 diagnostic levels of histopathology. As might be expected, earlier disease was more difficult to differentiate than late disease in the current study (AUCs of 0.82 vs. 0.93). Likewise, if dysplastic lesions are excluded from the current analysis, the diagnostic performance becomes optimistic (AUCs of 0.97 and 0.95 for 1 vs. 6 and 2 vs. 6, respectively). Although there was a small proportion of false-negative results warranting further investigation, these results were consistent with the imperfection of diagnostic adjuncts and suggest that persistent mucosal lesions may necessitate subsequent resampling.

One limitation for the current study is that lesions were evaluated by expert clinicians in secondary care settings where the prevalence of high-grade OED and OSCC would be higher than in primary care. Further, subjects met strict inclusion

criteria, which may reflect a narrower spectrum of lesions than might be clinically diagnosed as OPMDs in a primary care setting. Because prevalence of high-grade OED and OSCC is expected to be substantially lower in primary care settings, future studies are needed to evaluate the diagnostic performance of OPMDs detected there.

In closing, this cytology-on-a-chip approach shows potential as an oral lesion precision diagnostic in various patient settings. Primary care clinicians typically do not have the information needed to effectively differentiate the significance of oral mucosal lesions. This automated cytology platform will help primary care clinicians perform a more accurate and real-time risk stratification of lesions, allowing them to make appropriate referrals. In secondary or tertiary care settings, the cytological signatures of patients with a history of OED and OSCC may be monitored longitudinally and have the potential to identify progression and malignant transformation/recurrence earlier, and less invasively, than current surveillance approaches. This tool may be further developed to identify unique cytological signatures for other mucosal diseases, whether immune (e.g., lichen planus) or pathogen-mediated (e.g., candidal leukoplakia). Plans are now in place to validate and assess diagnostic performance versus routine care in primary care clinics. Although the same technology has shown preliminary promise for detecting disease progression and regression over a 2-y period in patients with Fanconi anemia (Abram et al. 2018), additional plans are in place to follow high-risk patients longitudinally for malignant transformation and cancer recurrence in secondary or tertiary surveillance settings.

Author Contributions

M.P. McRae, contributed to conception, design, data acquisition, analysis, and interpretation, drafted and critically revised the manuscript; A.R. Kerr, M.H. Thornhill, S.W. Redding, N. Vigneswaran, contributed to design, data acquisition, and interpretation, critically revised the manuscript; M.N. Janal, S.K. Kang, R. Niederman, contributed to data analysis and interpretation, critically revised the manuscript; N.J. Christodoulides, D.A. Trochesset, I. Dapkins, contributed to data interpretation, critically revised the manuscript; C. Murdoch, J. Bouquot, S.S. Modak, G.W. Simmons, contributed to data acquisition, critically revised the manuscript; J.T. McDevitt, contributed to conception, design, data acquisition, analysis, and interpretation, critically revised the manuscript. All authors gave final approval and agree to be accountable for all aspects of the work.

Declaration of Conflicting Interests

The authors declared the following potential conflicts of interest with respect to the research, authorship, and/or publication of this article: M.P. McRae has served as a paid consultant for SensoDx and has a provisional patent pending. G.W. Simmons has patents US10060937B2 and US7781226B2 issued. D.A. Trochesset has received grants from the New York University College of Dentistry for work performed as part of the current study. M.H. Thornhill has received National Institutes of Health grant 1RC2DE020785-01 for work performed as part of the current study. S.W. Redding has patent US9535068B2 issued. S.K. Kang has received royalties from Wolters Kluwer and honoraria from the *American Journal of Roentgenology* for work performed outside of the current study. J.T. McDevitt has received grants from the National Institutes of Health for work performed as part of the current study (grants 1RC2DE020785-01, 4R44DE025798-02, and R01DE024392) and has a provisional patent pending. In addition, he has ownership positions and equity interest in both SensoDx II LLC and OraLiva, Inc. All other authors declare no potential conflicts of interest with respect to the authorship and/or publication of this article.

ORCID iDs

M.P. McRae https://orcid.org/0000-0002-2126-9442

M.H. Thornhill https://orcid.org/0000-0003-0681-4083

C. Murdoch https://orcid.org/0000-0001-9724-122X

References

Abram TJ, Floriano PN, Christodoulides N, James R, Kerr AR, Thornhill MH, Redding SW, Vigneswaran N, Speight PM, Vick J, et al. 2016. "Cytology-on-a-chip" based sensors for monitoring of potentially malignant oral lesions. Oral Oncol. 60:103–111.

Abram TJ, Pickering CR, Lang AK, Bass NE, Raja R, Meena C, Alousi AM, Myers JN, McDevitt JT, Gillenwater AM, et al. 2018. Risk stratification of oral potentially malignant disorders in Fanconi anemia patients using autofluorescence imaging and cytology-on-a chip assay. Transl Oncol. 11(2):477–486.

Akobeng AK. 2007. Understanding diagnostic tests 2: likelihood ratios, pre- and post-test probabilities and their use in clinical practice. Acta Paediatr. 96(4):487–491.

Babshet M, Nandimath K, Pervatikar S, Naikmasur V. 2011. Efficacy of oral brush cytology in the evaluation of the oral premalignant and malignant lesions. J Cytol. 28(4):165–172.

Belin BJ, Cimini BA, Blackburn EH, Mullins RD. 2013. Visualization of actin filaments and monomers in somatic cell nuclei. Mol Biol Cell. 24(7):982–994.

de Jong EP, Xie H, Onsongo G, Stone MD, Chen X-B, Kooren JA, Refsland EW, Griffin RJ, Ondrey FG, Wu B, et al. 2010. Quantitative proteomics reveals myosin and actin as promising saliva biomarkers for distinguishing pre-malignant and malignant oral lesions. PLoS One. 5(6):e11148.

El-Naggar AK, Chan JK, Grandis JR, Takata T, Slootweg PJ, editors. 2017. Who classification of tumours of the head and neck. Lyon (France): IARC Press.

Gunning P, O'Neill G, Hardeman E. 2008. Tropomyosin-based regulation of the actin cytoskeleton in time and space. Physiol Rev. 88(1):1–35.

Hemstreet GP 3rd, Rao J, Hurst RE, Bonner RB, Waliszewski P, Grossman HB, Liebert M, Bane BL. 1996. G-actin as a risk factor and modulatable endpoint for cancer chemoprevention trials. J Cell Biochem Suppl. 25:197–204.

Huber MA. 2018. Adjunctive diagnostic techniques for oral and oropharyngeal cancer discovery. Dent Clin North Am. 62(1):59–75.

Le HQ, Ghatak S, Yeung C-YC, Tellkamp F, Günschmann C, Dieterich C, Yeroslaviz A, Habermann B, Pombo A, Niessen CM, et al. 2016. Mechanical regulation of transcription controls Polycomb-mediated gene silencing during lineage commitment. Nat Cell Biol. 18(8):864–875.

Lingen MW, Abt E, Agrawal N, Chaturvedi AK, Cohen E, D'Souza G, Gurenlian J, Kalmar JR, Kerr AR, Lambert PM, et al. 2017. Evidence-based clinical practice guideline for the evaluation of potentially malignant disorders in the oral cavity: a report of the American Dental Association. J Am Dent Assoc. 148(10):712–727.

McRae MP, Modak SS, Simmons GW, Trochesset DA, Kerr AR, Thornhill MH, Redding SW, Vigneswaran N, Kang SK, Christodoulides NJ, et al. 2020. Point-of-care oral cytology tool for the screening and assessment of potentially malignant oral lesions. Cancer Cytopathol. 128(3):207–220.

Miroshnikova YA, Nava MM, Wickström SA. 2017. Emerging roles of mechanical forces in chromatin regulation. J Cell Sci. 130(14):2243–2250.

Moore HM, Vartiainen MK. 2017. F-actin organizes the nucleus. Nat Cell Biol. 19(12):1386–1388.

Olson MF, Sahai E. 2009. The actin cytoskeleton in cancer cell motility. Clin Exp Metastasis. 26(4):273–287.

Pereira LHM, Reis IM, Reategui EP, Gordon C, Saint-Victor S, Duncan R, Gomez C, Bayers S, Fisher P, Perez A, et al. 2016. Risk stratification system for oral cancer screening. Cancer Prev Res (Phila). 9(6):445–455.

Poate TWJ, Buchanan JAG, Hodgson TA, Speight PM, Barrett AW, Moles DR, Scully C, Porter SR. 2004. An audit of the efficacy of the oral brush biopsy technique in a specialist oral medicine unit. Oral Oncol. 40(8):829–834.

Rashid A, Warnakulasuriya S. 2015. The use of light-based (optical) detection systems as adjuncts in the detection of oral cancer and oral potentially malignant disorders: a systematic review. J Oral Pathol Med. 44(5):307–328.

Sciubba JJ. 1999. Improving detection of precancerous and cancerous oral lesions: computer-assisted analysis of the oral brush biopsy. J Am Dent Assoc. 130(10):1445–1457.

Speight PM, Abram TJ, Floriano PN, James R, Vick J, Thornhill MH, Murdoch C, Freeman C, Hegarty AM, D'Apice K, et al. 2015. Interobserver agreement in dysplasia grading: toward an enhanced gold standard for clinical pathology trials. Oral Surg Oral Med Oral Pathol Oral Radiol. 120(4):474–482.

Stevenson RP, Veltman D, Machesky LM. 2012. Actin-bundling proteins in cancer progression at a glance. J Cell Sci. 125(Pt 5):1073–1079.

Svirsky JA, Burns JC, Carpenter WM, Cohen DM, Bhattacharyya I, Fantasia JE, Lederman DA, Lynch DP, Sciubba JJ, Zunt SL. 2002. Comparison of computer-assisted brush biopsy results with follow up scalpel biopsy and histology. Gen Dent. 50(6):500–503.

Tampa M, Mitran MI, Mitran CI, Sarbu MI, Matei C, Nicolae I, Caruntu A, Tocut SM, Popa MI, Caruntu C, et al. 2018. Mediators of inflammation—a potential source of biomarkers in oral squamous cell carcinoma. J Immunol Res. 2018:1061780.

Warnakulasuriya S, Reibel J, Bouquot J, Dabelsteen E. 2008. Oral epithelial dysplasia classification systems: predictive value, utility, weaknesses and scope for improvement. J Oral Pathol Med. 37(3):127–133.

Weigum SE, Floriano PN, Redding SW, Yeh C, Westbrook SD, McGuff HS, Lin A, Miller FR, Villarreal F, Rowan SD, et al. 2010. Nano-bio-chip sensor platform for examination of oral exfoliative cytology. Cancer Prev Res (Phila). 3(4):518–528.